Stability Analysis of a Microgrid System based on Inverter-Interfaced Distributed Generators

Fabio ANDRADE[1], Konstantinos KAMPOUROPOULOS[2], Jordi CUSIDO[2], Luis ROMERAL[1]
[1]*Universitat Politècnica de Catalunya, 08222, Spain*
[2]*Fundació CTM Centre Tecnològic, 08242, Spain*
fabio.andrade@mcia.upc.edu

***Abstract*—This paper presents a phase-plane trajectory analysis and the appliance of Lyapunov´s methodology to evaluate the stability limits of a small signal model of a Microgrid system. The work done is based on a non-linear tool and several computer simulations. The study indicates how to analyze a Microgrid system that is subjected to a severe transient disturbance by using its large signal model without the necessity of the small signal analysis as it is commonly applied.**

***Index Terms*—Lyapunov method, microgrid systems, parallel inverters, small-signal stability, transient stability.**

I. INTRODUCTION

Intelligent Microgrids integrate different energy resources, especially renewable sources, to provide dependable and efficient operations while they work on-grid connection or on islanding mode. They can ensure an uninterrupted reliable flow of power, offering economic and environmental benefits and minimizing the energy loss through the transmission over long distances. The use of systems of local power generation and storage allow to the grid and the critical facilities to operate independent of the public utility when this is necessary and thus to eliminate possible blackouts in the system. New technologies of Microgrids can automatically fix and even anticipate the power disturbances. They can also supply energy to the public utility when their generated power is higher that the demand of their loads or when the selling price is convenient. In order use all the capabilities and advantages that the Microgrids can offer, the use of intelligent power interfaces between the renewable source and the grid are required. These interfaces have as final element a dc/ac inverter which can be classified as current source inverter (CSI) or voltage-source inverter (VSI) as it is detailed presented in [1-2].

On the existed interfaces, there are control topologies, where the use of a master control for the inverters is not required. In those topologies, a main advantage is that each inverter is able to change the voltage and frequency of the Microgrid depending of the actual PQ power flow of it. Besides that, a fault of an inverter does not cause a collapse of the whole system. In fact, each inverter could be act as a plug-and-play entity to make the Microgrid an expandable system. The communication between the inverters is not necessary for the stability of the system but it can be used to improve its performance [3].

In these interfaces, the active and reactive shared powers inside the local grid are managed by a dc/ac converter with a decentralized control system. This system is part of a main control structure with a hierarchical topology. This control consists of three levels and divides the tasks in order to improve the smartness of the Microgrid [4]. The lower level of the control consists of two loops, an inner and an outer. The inner loop is used for the current and voltage regulation while the outer loop uses the PQ droop curves and the virtual impedance to share the active and the reactive power to the loads using only the control´s local variables [5]. A second level copes with the synchronization or the islanding algorithms [6-8]; this control works in the point of common coupling. Finally the tertiary control deals with the energy management, the electrical market and the energy exchange with the utility (importation and exportation) [9].

This hierarchical control strategy allows the inverters to share the demanded active and reactive power in the Microgrid according to their maximum operation ranges.

As far as stability issues are concerned, a completed roots locus analysis, Nyquist and Bode studies have been previously reported [10-13]. Most of these research works are based on dynamical models with a large number of state variables and neglected dynamics in the DC link. Because of the complexity of these models, it is necessary to use some assumptions and reduced field tools, such as small signals and others to perform an analysis.

In large signal analysis, Lyapunov functions are used to control the current, maintaining the stability of the system [14-16]. These strategies facilitate the current control of such inverters directly in the abc-frame.

This paper works with both lineal and non-lineal tools for large signal analysis that is supported by computer simulations. It uses phase-plane trajectory analysis and the Lyapunov methodology to determine the stability of the system in large disturbance. It suggests the utilization of a new model presenting how to analyze the system when it is subjected to a severe transient disturbance, such as loss of large loads or loss of generation.

The outline of the paper is as follows. Firstly, the topology of the Microgrid and its basic equations are described. Then, the mathematical model of the Microgrid is analyzed in state variables and the equilibrium point of the system is found. Finally the implementation of the methodology is applied, presenting different simulations of the system and commenting the main conclusions of the study.

Digital Object Identifier 10.4316/AECE.2013.03003

II. Study of the Microgrid System

A typical Microgrid system in stand-alone mode based in parallel inverters is presented in Fig. 1. It is assumed that this system is a balanced three-phase circuit.

Each generator consists of a DC power renewable source, a DC/AC inverter and a low pass filter and it is managed by two control loops. The inner loop is used to regulate the output voltage and current while the outer loop is used to control the shared power and trade-off the PQ power in the Microgrid without the use of any communication between the generators. The model does not consider the dynamics of the inner loop because of their high frequency behavior. This simplification has been studied and been presented in [17-18].

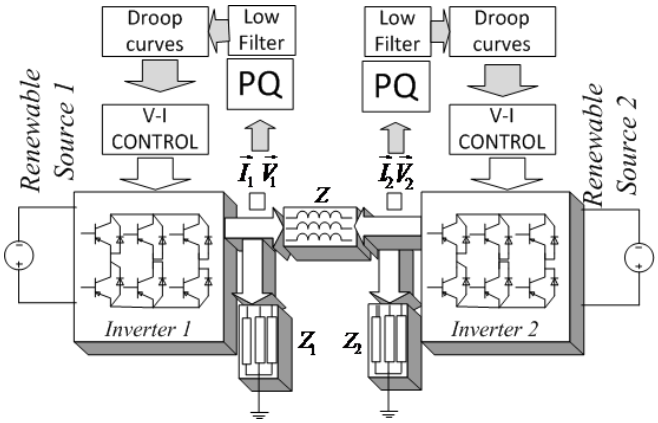

Figure 1. Typical structure of a Microgrid system based on inverters.

The different voltage signals of the system can be represented as follows, as they are depicted in Fig 1.

$$V_1 = \overline{V}_1 e^{j\theta_1};\quad V_2 = \overline{V}_2 e^{j\theta_2};\quad \theta_{12} = \theta_1 - \theta_2$$
$$\overline{V}_i = \frac{V_{\max}}{\sqrt{2}};\quad \theta_i = \arctan\left(\frac{v_{qi}}{v_{di}}\right) \tag{1}$$

The following equation describes the impedances Z1, Z2 and Z3.

$$Z_1 = \overline{Z}_1 e^{j\theta_{Z_1}};\quad Z_2 = \overline{Z}_2 e^{j\theta_{Z_2}};\quad Z_3 = \overline{Z}_3 e^{j\theta_{Z_3}}$$
$$\overline{Z}_i = \sqrt{R_i^2 + (\omega L_i)^2};\quad \theta_{Z_i} = \tan^{-1}\left(\frac{\omega L_i}{R_i}\right) \tag{2}$$

The PQ controller uses an artificial droop control scheme with average signals of P and Q which are obtained using the low-pass filter. The artificial droop's equations can be expressed as:

$$\omega_i - \omega_0 = -k_p P \qquad V_i - V_0 = -k_v Q \tag{3}$$

A low-pass filter is used to generate the average values of the active and reactive power and it is described in the equation (4). The cut-off frequency (ω_f) is a decade lower than the Microgrid frequency.

$$P(s) = \frac{\omega_f}{s+\omega_f} P_i(s) \quad Q(s) = \frac{\omega_f}{s+\omega_f} Q_i(s) \tag{4}$$

To calculate the instantaneous three-phase power, a per phase analysis is applied:

$$p_{3\phi}(t) = v_a(t) i_a(t) + v_b(t) i_b(t) + v_c(t) i_c(t)$$
$$p_{3\phi}(t) = \overline{V} \cdot \overline{I}\left[3\cos(\phi) + \cos(2\omega t + \varphi) + \cos(2\omega t + \varphi - 120)\cos(2\omega t + \varphi + 120)\right] \tag{5}$$

where ϕ is the angle between the V and I phasors.

The equation (6) presents the calculation of the three-phase power after the cancelation of the double-frequency terms.

$$p_{3\phi}(t) = 3\overline{V} \cdot \overline{I}\cos(\phi) \tag{6}$$

The system shown in Fig. 1 uses the parameters presented in Table I.

TABLE I. System Parameters

Variable	Size	Style
Operating Voltage range	218,5 – 241,5	*Vrms*
Operating Frequency range	49 - 51	*Hz*
Z - Line transmission Inductance	5	*mH*
Z_1 - Resistor R_1 - Inductor $_{L1}$	150 - 10	*Ω - mH*
Z_2 - Resistor R_2 - Inductor L_2	120 - 50	*Ω - mH*
Frequency droop coefficient (K_{p1}=K_{p2})	1,33e-4	$rad.s^{-1}/W$
Voltage droop coefficient (K_{v1}=K_{v2})	0.0015	*V/VAR*
Cutoff frequency filter	5	*Hz*

III. A Mathematical Model

A mathematical model of a simple 3-phases balanced system is considered to analyze the transient stability of the system. The method of per phase analysis is used in order to calculate the complex power. The per-phase electrical circuit of the balanced system is depicted in Fig. 2. Each generator has a shared (S_{12} or S_{21}) and a local power (S_{L1} or S_{L2}). The power angle between both generators can be defined as:

$$\dot{\theta}_{12} = \omega_1 - \omega_2 \tag{7}$$

The following equation describes the complex power that is generated by each DG.

$$S_1 = S_{L1} + S_{12} \quad , \quad S_2 = S_{L2} + S_{21} \tag{8}$$

Where S_{12} (or S_{21}) is the complex power generated by DG_1 (or DG_2) and supplied to the transmission line that is connected to the DG_2 (or DG_1) and S_{Li} is the local complex power. The complex powers are defined as:

$$P_1 = \left(67\times10^{-4}\right)\overline{V}_1^2 - 0.63\overline{V}_1\overline{V}_2\sin(\theta_{12})$$
$$P_2 = \left(82\times10^{-4}\right)\overline{V}_2^2 - 0.63\overline{V}_1\overline{V}_2\sin(\theta_{12}) \tag{9}$$
$$Q_1 = \left(1.4\times10^{-4}\right)\overline{V}_1^2 + 0.63\overline{V}_1^2 - 0.63\overline{V}_1\overline{V}_2\cos(\theta_{12})$$
$$Q_2 = \left(11\times10^{-4}\right)\overline{V}_2^2 + 0.63\overline{V}_2^2 - 0.63\overline{V}_1\overline{V}_2\cos(\theta_{12})$$

It is possible to rewrite the curve droop equation and the low pass filter in the time domain as follows:

$$\dot{\omega}_i = 9.8\times10^3 - 31.4\omega_i - 0.0042P_i$$
$$\dot{V}_i = 7.2\times10^3 - 31.4V_i - 0.0482Q_i \tag{10}$$

Using a state-space representation of the combined equations of (9) and (10), it concludes that:

$$f(X_i) = \dot{X}_i \quad i = 1,2...,5$$
$$\dot{X}_1 = X_2 - X_3$$
$$\dot{X}_2 = \alpha_1 - \alpha_2 X_2 - \alpha_4 X_4^2 - \alpha_3 X_4 X_5 \sin(X_1)$$
$$\dot{X}_3 = \alpha_1 - \alpha_2 X_3 - \alpha_5 X_5^2 + \alpha_3 X_4 X_5 \sin(X_1) \tag{11}$$
$$\dot{X}_4 = \alpha_6 - \alpha_2 X_4 - \alpha_7 X_4^2 + \alpha_8 X_4 X_5 \cos(X_1)$$
$$\dot{X}_5 = \alpha_6 - \alpha_2 X_5 - \alpha_7 X_5^2 + \alpha_8 X_4 X_5 \cos(X_1)$$

Where:

$$\alpha_1 = 9.8\times10^3;\alpha_2 = 31.4;\alpha_3 = 0.0027;\alpha_4 = 2.8\times10^{-5}$$
$$\alpha_5 = 3.4\times10^{-5};\alpha_6 = 7.2\times10^3;\alpha_7 = 0.031;\ \alpha_8 = 0.031$$

This model permits to consider a large variation of the angle between the generators.

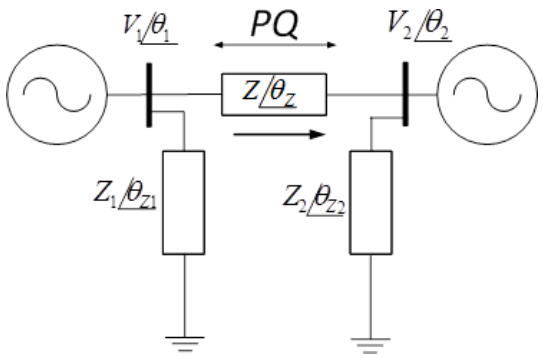

Figure 2. Per phase electrical circuit of the whole system (Z_1= 150.03Ω, θ_{Z1}= 0.021Rad, Z_2= 121.02Ω, θ_{Z2}= 0.13Rad, Z= 1.57Ω, θ_Z= 1.5708Rad)

IV. Equilibrium Points

The equilibrium points can be obtained, cancelling all the derivatives of the system (equal to zero):

$$
\begin{aligned}
&f(X_i)=0\\
&0=X_2-X_3\\
&0=\alpha_1-\alpha_2X_2-\alpha_4X_4^2-\alpha_3X_4X_5\sin(X_1)\\
&0=\alpha_1-\alpha_2X_3-\alpha_5X_5^2+\alpha_3X_4X_5\sin(X_1)\\
&0=\alpha_6-\alpha_2X_4-\alpha_7X_4^2+\alpha_8X_4X_5\cos(X_1)\\
&0=\alpha_6-\alpha_2X_5-\alpha_7X_5^2+\alpha_8X_4X_5\cos(X_1)
\end{aligned}
\qquad (12)
$$

Where: $X_1=\theta_{12};X_2=\omega_1;X_3=\omega_2;X_4=\overline{V}_1;X_5=\overline{V}_2$

Using mathematical software to solve the equation (12) the equilibrium points X_{0i}=*[X_{01} X_{02} X_{03} X_{04} X_{05}]* have been calculated and depicted in Fig. 3. In the range of the state variable X_5 there is an equilibrium point at X_0 = *[0.0019 320.18 320.18 239.7 239.6]*.

V. Stability of the System

The transient stability still remains a basic and important consideration in the design of power systems [19]. There are different forms of instabilities that a power system may undergo. It is possible to use the mathematical model to analyze the stability by mean of controlled stages. The model can be adapted for each stage in order to obtain the angle and the voltage stabilities.

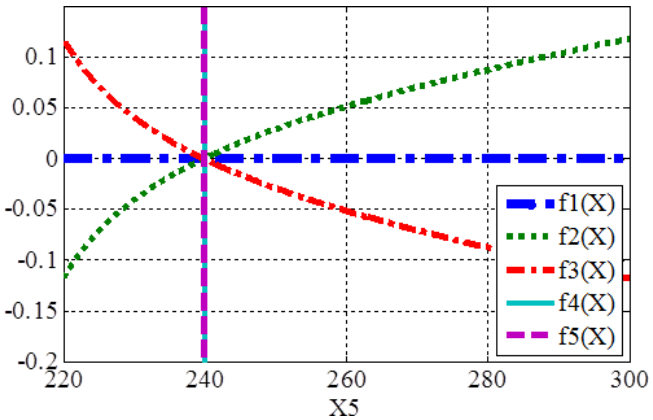

Figure 3. The equilibrium point X_0=*[0.0019 320.1 320.1 239.7 239.6]* in the range of the variable X_5.

A. Analysis of the equilibrium point and small-signal stability

The stability of the equilibrium point X_0 can be determined via linearization [20-21]. Applying the Jacobian matrix of *f(X)* at the equilibrium point concludes that:

$$
A=\begin{bmatrix} a_{11} & \cdots & a_{15}\\ \vdots & \ddots & \vdots\\ a_{51} & \cdots & a_{55}\end{bmatrix}=\begin{bmatrix} \frac{\partial f_1(X)}{\partial X_1} & \cdots & \frac{\partial f_1(X)}{\partial X_5}\\ \vdots & \ddots & \vdots\\ \frac{\partial f_5(X)}{\partial X_5} & \cdots & \frac{\partial f_5(X)}{\partial X_5}\end{bmatrix}_{X0} \qquad (13)
$$

The values of the *A* matrix are:

$$
A=\begin{bmatrix} 0.0000 & 1.0000 & -1.000 & 0.0000 & 0.0000\\ -153.9 & -32.04 & 0.0000 & -0.0145 & -0.0009\\ 153.90 & 0.0000 & -32.04 & -0.0009 & -0.0162\\ -2.363 & 0.0000 & 0.0000 & -39.407 & 7.3597\\ -2.363 & 0.0000 & 0.0000 & 7.3599 & -39.407\end{bmatrix} \qquad (14)
$$

And the respective eigenvalues are:

$\lambda_{1,2}=-16.02\pm i7.1;\ \lambda_3=-32.05;\ \lambda_4=-46.8;\lambda_5=-32.05$

It can be observed that all the eigenvalues are negative concluding that the equilibrium point is stable in small signal. Figure 4 shows the variation of the equilibrium point and their eigenvalues when a variation appears in the frequency droop coefficient from 1.3e-3 to 7.8e-4. Although the system is stable, the damping is poorer when the frequency droop coefficient increases.

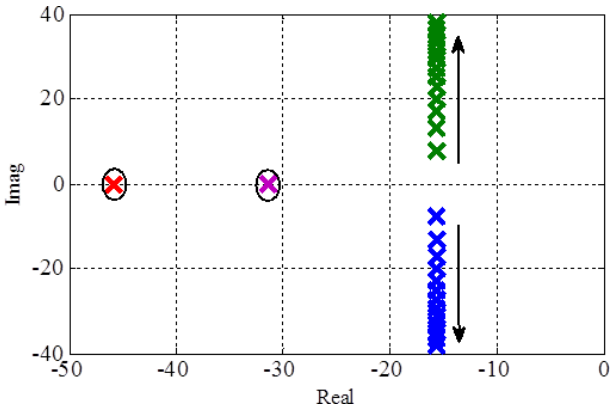

Figure 4. Root locus for 1.3e-4< Kp <7.8e-4.

B. Analysis of the Lyapunov methodology for the system´s stability

In order to analyze the system´s stability by applying the Lyapunov's methodology, a single generator has been considered. To test the behavior of the system, a series of variation only in the angle, in the active power and in the frequency have been done. The variation in the voltage was negligence. The set of equation for the single generator is given by:

$$
f(Y)=\begin{cases}\dot{Y}_1=Y_2-100\pi\\ \dot{Y}_2=9.8\times10^3-31.4Y_2-2.8\times10^{-5}Y_3^2-0.62Y_3\sin(Y_1)\\ \dot{Y}_3=7.2\times10^3-31.4Y_3-0.0307Y_3^2+7.061Y_3\cos(Y_1)\end{cases} \qquad (15)
$$

Equation (15) reaches the equilibrium point given by the solution of the nonlinear algebraic equation $f(Y)=0$. The solutions of this equation in a voltage generator interval of 180 to 260Vrms are Y_{01}=*[-1.5643 314.1593 194.0400]* and Y_{02}=*[-0.0105 314.1593 229.9900]*.

It is easy verified by linearization of (15) that Y_{02} is the stable and Y_{01} is the unstable equilibrium points. For

Lyapunov stability analysis is convenient to transfer the stable equilibrium point to the origin by the transformation: $Z=Y-Y_{02}$

Thus, (14) becomes:

$$\begin{aligned}\dot{Z}_1 &= Z_2\\ \dot{Z}_2 &= -1.47-31.4Z_2-2.8\times10^{-5}Z_3^2-0.01Z_3+\\ &\quad 0.006Z_3\sin(Z_1)-0.6Z_3\cos(Z_1)-140\sin(Z_1)+\\ &\quad 1.47\cos(Z_1)\\ \dot{Z}_3 &= -1.6\times10^3-13.8Z_3-0.03Z_3^2-6.9Z_3\cos(Z_1)+\\ &\quad 0.07Z_3\cos(Z_1)+1.6\times10^3\cos(Z_1)+16.6\sin(Z_1)\end{aligned} \quad (16)$$

This study case considers that the system is working in the stable equilibrium point and there is a large variation in the angle (Z_1). Taking into account that the voltage magnitude is constant, it is possible to work with the reduced model (17).

$$\begin{aligned}\dot{Z}_1 &= Z_2\\ \dot{Z}_2 &= -31.4Z_2-f(Z_1)\end{aligned} \quad (17)$$

where $f(Z_1)=1.47+140\sin(Z_1)-1.47\cos(Z_1)$

The phase portrait of the reduced model is shown on Fig. 5. It can be observed that all the trajectories between -3 and 3 moves toward the equilibrium point at the origin.

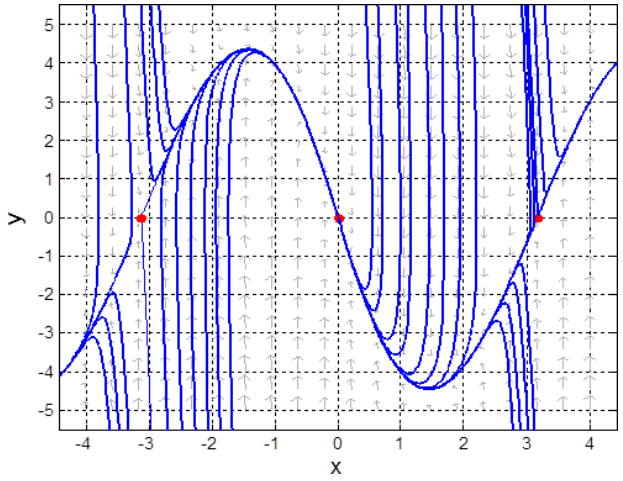

Figure 5. Phase portrait in Z_1–Z_2. ($x=Z_1$ $y=Z_2$).

A variable gradient method for constructing a Lyapunov function has been used as it is described in [22] and [23]. Applying the methodology to the equation (16), we obtain the Lyapunov function described as:

$$V(Z_1,Z_2)=\frac{1}{2}(31.4Z_1+Z_2)^2+\int_0^{Z_1}f(u)du \quad (18)$$

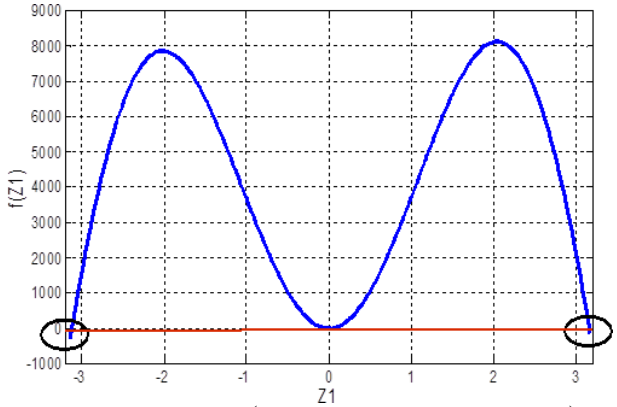

Figure 6. Function: $-31.4Z_1(1.47+140\sin(Z_1)-1.47\cos(Z_1))$

In order to verify that the region $V(Z_1,Z_2)<V(\pi-Z_{01})$ is asymptotic stable, the derivative of the equation (18) is calculated as: $\dot{V}(Z_1,Z_2)=-31{,}4f(Z_1)Z_1$. The region is depicted in Fig 6.

VI. Simulations Result

The proposed Microgrid was simulated in order to show the behavior of the system and its equilibrium points. Fig 7 shows a simulation file carried out in MATLAB/Simulink by means of POWER ELECTRONICS TOOLBOX.

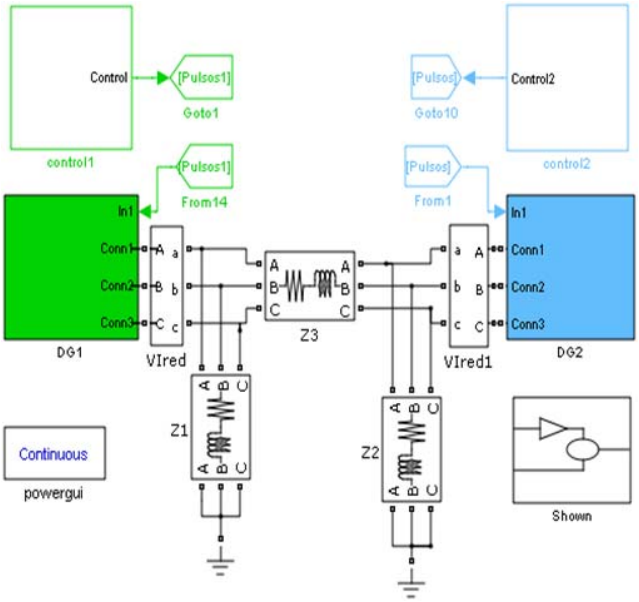

Figure 7. Microgrid carried out in MATLAB/SIMULINK.

Figure 8 shows the angle difference between the voltages of each generator. In this case, it is assumed that all the DGs and impedances parameters, given in Table I, are considered. There are no faults during the operating.

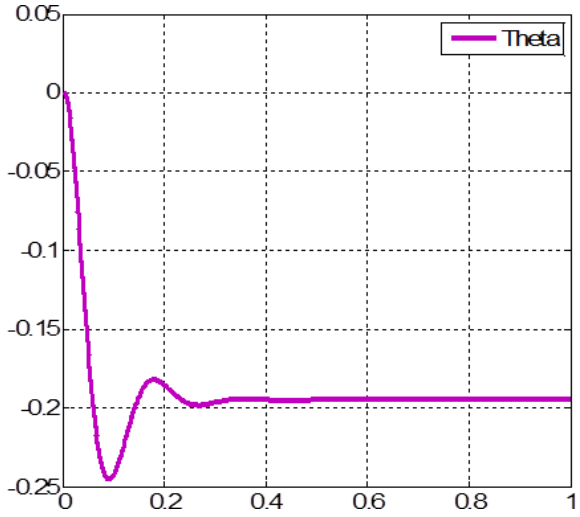

Figure 8. Angle difference between the voltages V_1 and V_2

When the system begins, the angle between V_1 and V_2 is zero. It has a transient response and it reaches to steady point at 0.19 rad. All the derivatives of the equations in (12) take the value zero in the same instant when θ_{12}=0.19 *rad*, $\omega_1=\omega_2=2\pi(50.96)$ rad/s, V_1=239.7 Vrms and V_2=239.6 Vrms.

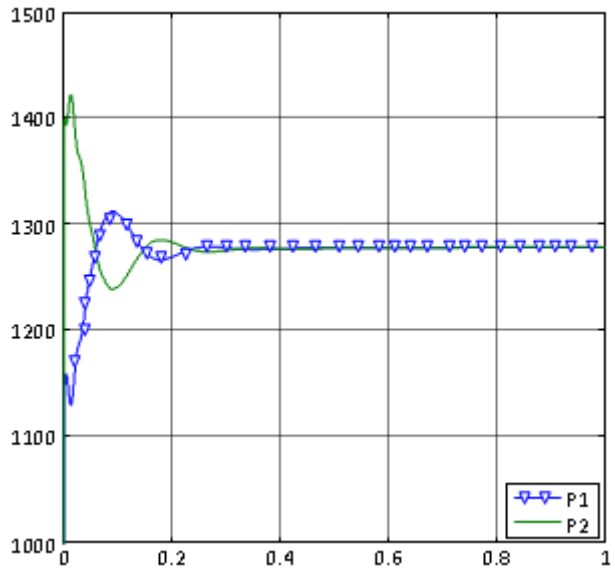

Figure 9. Active Power dispatch by each DG using the values of the Table I.

Figures 9 and 10 show the active and reactive power of each generator. The system reaches a steady state before the first second. The active and reactive power signals have a large percent overshoot (>25%).

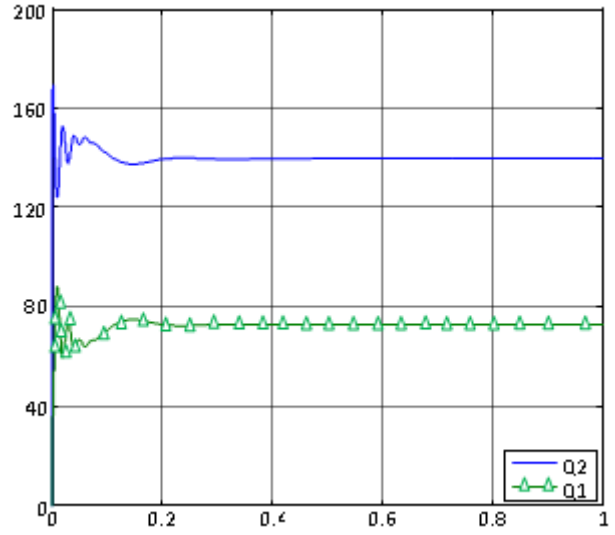

Figure 10. Reactive Power dispatch by each DG using the values of the Table I.

As discussed before in the study of stability section, the power sharing can be modified by choosing different droop controller gains. The eigenvalues analysis presents a poor damping for huge droop controller gains. Figure 11 shows the variation of the P power of a generator when the K_p coefficient increases.

Figure 12 shows two large disturbances in the Microgrid. The first disturbance happens at second 1 and has a duration of 0.2 seconds. After the disturbance, the Microgrid can be recovered successfully. The second event happens at the fourth second occurring a permanent loss of stability.

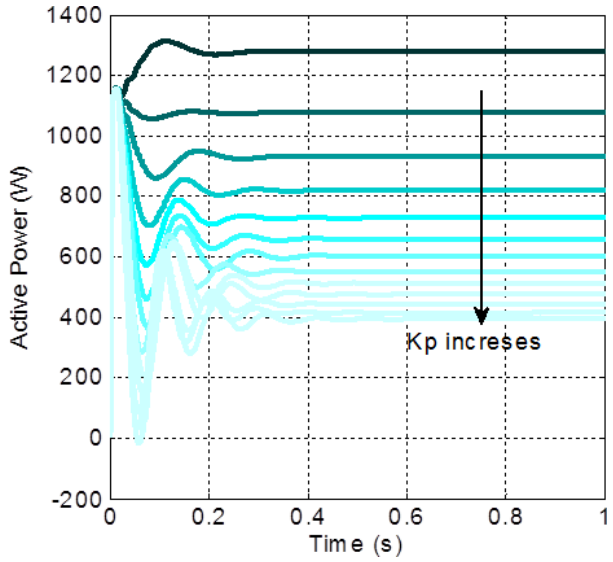

Figure 11. Active Power dispatch by DG 1 when the Kp increases.

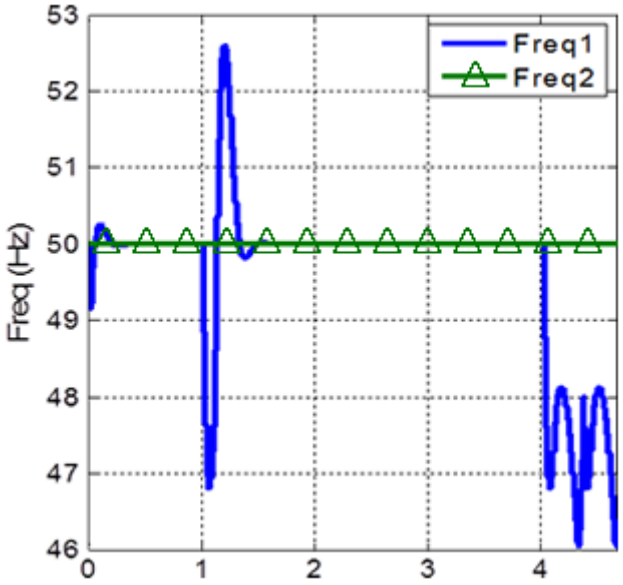

Figure 12a. Frequency variation of DG1, applying two large disturbances.

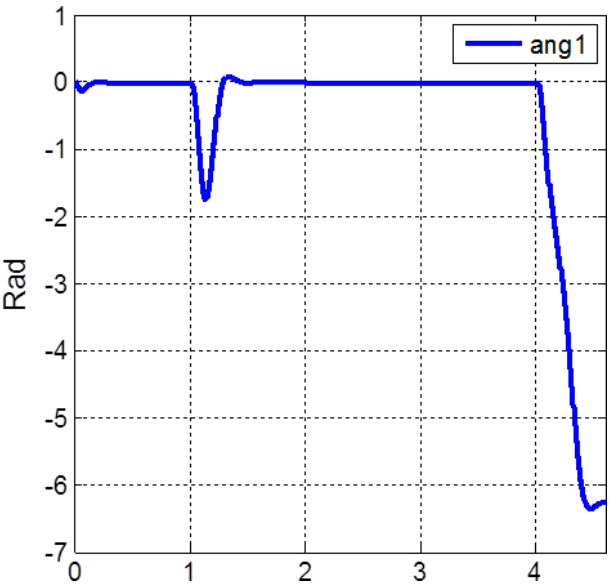

Figure 12b. Angle variation of DG1, applying two large disturbances.

VII. CONCLUSION

In this paper, a nonlinear state-space model of a Microgrid is presented. The model includes the most important dynamics. The no-linear model can find the equilibrium points. The model has been analyzed by means of two different studies; first, a study of small signal stability by mean of linearization and root locus plot and second, a transient stability by mean of Lyapunov function. The analysis shows that the studies of small signal could be useful to adjust the controller and improve the transient response and the steady-state error. Using the Lyapunov function, the region of asymptotic stability, the size of the disturbed and his duration time could be determined. These tools allow to design Microgrid systems with loads, generators and storage systems, assuring the global stability of them.

REFERENCES

[1] Dasgupta, S.; Mohan, S.N.; Sahoo, S.K.; Panda, S.K., "Application of Four-Switch-Based Three-Phase Grid-Connected Inverter to Connect Renewable Energy Source to a Generalized Unbalanced Microgrid System," Industrial Electronics, IEEE Transactions on , vol.60, no.3, pp.1204,1215, March 2013

[2] Soultanis N. L.: A Stability Algorithm for the Dynamic Analysis of Inverter Dominated Unbalanced LV Microgrids, IEEE Transactions on Power Systems, 2007, pp. 294 – 304.

[3] Shivkumar V. I.: A Generalized Computational Method to Determine Stability of a Multi Inverter Microgrid, IEEE Transactions on Power Electronics, 2010, pp. 2420 – 2432.

[4] J.M. Guerrero, J.C. Vasquez, J. Matas, L.G. de Vicuna, M. Castilla, "Hierarchical Control of Droop-Controlled AC and DC Microgrids—A General Approach Toward Standardization," IEEE Trans. Industrial Electronics, vol. 58, no 1, pp. 158–172, Jan. 2011.

[5] K. Jaehong, J.M. Guerrero, P. Rodriguez, R. Teodorescu, N. Kwanghee, "Mode Adaptive Droop Control With Virtual Output Impedances for an Inverter-Based Flexible AC Microgrid," IEEE Trans. Power Electron., vol. 26, no 3, pp. 689–701, Mar. 2011.

[6] B.Bahrani, H. Karimi, R. Iravani, "Nondetection Zone Assessment of an Active Islanding Detection Method and its Experimental Evaluation," IEEE Trans. Power Devivery, vol. 26, no 2, pp. 517–525, Mar. 2011.

[7] I.J. Balaguer, L. Qin, Y. Shuitao, U. Supatti, Z. P. Fang, "Control for Grid-Connected and Intentional Islanding Operations of Distributed Power Generation," IEEE Trans. Industrial Electronics, vol. 58, no 1, pp. 147–157, Jan. 2011.

[8] A. Samui, S.R. Samantaray, "Assessment of ROCPAD Relay for Islanding Detection in Distributed Generation," IEEE Trans. Smart Grid, vol. 2, no 2, pp. 391–398, Mar. 2011.

[9] C.Chen, S. Duan, T. Cai, B. Liu, G. Hu, "Smart Energy Management System for Optimal Microgrid Economic Operation," Renewable Power Generation, IET, vol. 5, no 3, pp. 258–267, May. 2011.

[10] Kasem Alaboudy, A.H.; Zeineldin, H.H.; Kirtley, J.L., "Microgrid Stability Characterization Subsequent to Fault-Triggered Islanding Incidents," Power Delivery, IEEE Transactions on , vol.27, no.2, pp.658,669, April 2012

[11] Turner, R.; Walton, S.; Duke, R., "A Case Study on the Application of the Nyquist Stability Criterion as Applied to Interconnected Loads and Sources on Grids," Industrial Electronics, IEEE Transactions on , vol.60, no.7, pp.2740,2749, July 2013

[12] Hao Liang; Bong Jun Choi; Weihua Zhuang; Xuemin Shen, "Stability Enhancement of Decentralized Inverter Control Through Wireless Communications in Microgrids," Smart Grid, IEEE Transactions on , vol.4, no.1, pp.321,331, March 2013

[13] Ashabani, S.M.; Mohamed, Y.A.I., "A Flexible Control Strategy for Grid-Connected and Islanded Microgrids With Enhanced Stability Using Nonlinear Microgrid Stabilizer," Smart Grid, IEEE Transactions on , vol.3, no.3, pp.1291,1301, Sept. 2012

[14] Dasgupta, S.; Mohan, S.N.; Sahoo, S.K.; Panda, S.K., "Lyapunov Function-Based Current Controller to Control Active and Reactive Power Flow From a Renewable Energy Source to a Generalized Three-Phase Microgrid System," Industrial Electronics, IEEE Transactions on , vol.60, no.2, pp.799,813, Feb. 2013

[15] Dasgupta, S.; Sahoo, S.K.; Panda, S.K., "Single-Phase Inverter Control Techniques for Interfacing Renewable Energy Sources With Microgrid—Part I: Parallel-Connected Inverter Topology With Active and Reactive Power Flow Control Along With Grid Current Shaping," Power Electronics, IEEE Transactions on , vol.26, no.3, pp.717,731, March 2011

[16] Lascu, C.; Asiminoaei, L.; Boldea, I.; Blaabjerg, F., "High Performance Current Controller for Selective Harmonic Compensation in Active Power Filters," Power Electronics, IEEE Transactions on , vol.22, no.5, pp.1826,1835, Sept. 2007

[17] Pogaku, N.: Modeling, Analysis and Testing of Autonomous Operation of an Inverter-Based Microgrid, IEEE Transactions on Power Electronics, 2007, pp. 613 – 625.

[18] Barklund, E.: Energy Management in Autonomous Microgrid Using Stability-Constrained Droop Control of Inverters, IEEE Transactions on Power Electronics, 2008, pp. 2346.

[19] Grigsby L. L.: Power System Stability and Control, CRC press, 2007, pp. 8-1.

[20] Coelho E. A. A.: Small-Signal Stability for Parallel-Connected Inverters in Stand-Alone AC Supply Systems, IEEE Transactions on Industry Applications, 2002, pp. 533 – 542.

[21] Diaz G.: Complex-Valued State Matrices for Simple Representation of Large Autonomous Microgrids Supplied by PQ and V f Generation, IEEE Transactions on Power Systems, pp. 1720-1730, 2009.

[22] Khalil H.: Nonlinear Systems. Prentice Hall, 1996, pp 200 - 225.

[23] Bacciotti A.: Lyapunov Function and Stability in Control Theory, Springer, 2005, pp. 27 – 80.